

High-Resolution Infrared Emission Spectrum of CaF

F. CHARRON, B. GUO, K.-Q. ZHANG, Z. MORBI, AND P. F. BERNATH

Centre for Molecular Beams and Laser Chemistry, Department of Chemistry, University of Waterloo, Waterloo, Ontario, Canada N2L 3G1

The high-resolution infrared emission spectrum of calcium monofluoride has been observed with a Fourier transform spectrometer. A total of 790 rovibrational transitions, from the $v = 1 \rightarrow 0$ to $v = 8 \rightarrow 7$ bands have been assigned. This set of infrared data has been combined with existing microwave data to yield improved Dunham Y_{ij} coefficients for the $X^2\Sigma^+$ electronic ground state of CaF. © 1995 Academic Press, Inc.

INTRODUCTION

CaF has enjoyed a renewed interest in recent years primarily due to its potential astrochemical importance and in the study of Rydberg states. The existing work on CaF has almost exclusively been the study of optical transitions by various spectroscopic techniques. The rotational analysis of the $A^2\Pi-X^2\Sigma^+$ transition has been extensively studied using laser excitation (1), microwave–optical double resonance (2), and intermodulated fluorescence (3) spectroscopy. The analysis of nine bands of the $B^2\Sigma^+-X^2\Sigma^+$ transition by Dulick *et al.* (4), of the 0–0 band of the $C^2\Pi-X^2\Sigma^+$ system by Ernst *et al.* (5), and of both the $E^2\Sigma^+-A^2\Pi$ and $E'^2\Pi^+-A^2\Pi$ transitions by Bernath and Field (6) has also been carried out using similar methods. More recently the characterization of the $B'^2\Delta$ state was performed by Vergès *et al.* (7) using a Fourier transform spectrometer to detect krypton-ion laser-induced fluorescence. In addition, Childs *et al.* have measured an electric dipole moment of 3.07 D in the CaF $X^2\Sigma^+$ ($v = 0$) ground state (8), as well as the v and N dependence of the spin–rotation and hyperfine interactions (9, 10).

With the recent confirmation of the detection of AlF toward the circumstellar envelope of the carbon star IRC + 10216 (11), Anderson *et al.* (12) recorded and analyzed the pure rotational spectrum of CaF in the four lowest vibrational levels of its ground state. Since calcium and aluminum have similar cosmic abundances, CaF may be detected in similar environments.

There has been extensive work on the Rydberg states of CaF by Field and co-workers (13–16). The large dipole moment of the CaF^+ ion-core causes extensive l -mixing of the Rydberg states, and CaF serves as a prototypical example of this type of Rydberg energy level pattern. In this paper, we present the first observation and analysis of the Fourier transform infrared emission spectrum of CaF.

EXPERIMENTAL DETAILS

The high-resolution infrared emission spectrum of CaF was observed with a Bruker IFS 120 HR Fourier transform spectrometer. The gas-phase CaF was produced by heating CaF_2 powder to a temperature of 1600°C in a commercial CM Rapid Temp

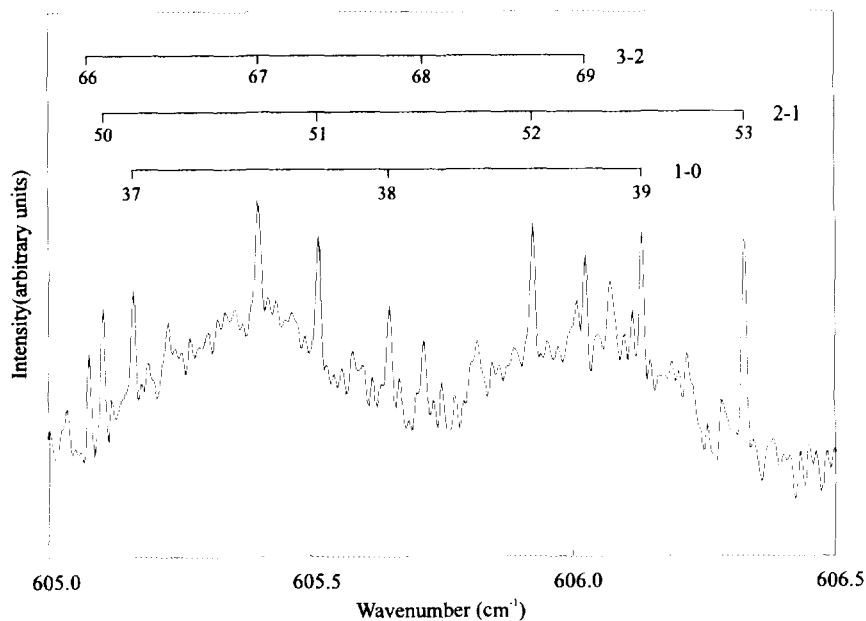


FIG. 1. A portion of the R branch of the vibration-rotation spectrum of CaF. The 1-0, 2-1, and 3-2 bands are marked along with the N'' value.

Furnace. The cell design consisted of an alumina (Al_2O_3) tube 1.2 m in length protected inside by a carbon liner. The tube was centered in the furnace and slowly brought up to the operating temperature at a rate of $200^\circ\text{C}/\text{hr}$. Impurities were removed from the system by pumping on the cell up to a temperature of 1000°C . Argon buffer gas

TABLE I

Dunham Coefficients for the $X^2\Sigma^+$ Ground State of CaF

Dunham Coefficient	Value (cm^{-1})
Y_{10}	588.67608(29)
Y_{20}	-2.91259(12)
$10^3 Y_{30}$	8.514(20)
$10^6 Y_{40}$	-6.1(11)
Y_{01}	0.3437181(12)
$10^3 Y_{11}$	-2.444671(93)
$10^6 Y_{21}$	4.917(20)
$10^8 Y_{31}$	2.77(12)
$10^7 Y_{02}$	-4.6954(20)
$10^{10} Y_{12}$	-1.29(11)
$10^{11} Y_{22}$	2.37(12)

TABLE II

Observed Rovibrational Line Positions of the $X^2\Sigma^+$ State of CaF in cm^{-1} [Observed-Calculated Values Are Shown in the Column Labeled Δ (in Units of 10^{-4}cm^{-1})]

1 0 Band				2 1 Band				3 2 Band			
N'	N''	Observed	Δ	N'	N''	Observed	Δ	N'	N''	Observed	Δ
67	68	525.7646	-8	67	68	520.3938	-13	57	58	524.6208	-6
66	67	526.7509	-2	65	66	522.3485	-13	56	57	525.5521	-12
65	66	527.7304	-22	63	64	524.2887	7	55	56	526.4810	-0
64	65	528.7105	5	62	63	525.2499	-12	54	55	527.4041	-4
63	64	529.6839	6	61	62	526.2097	-1	53	54	528.3234	-4
62	63	530.6538	13	60	61	527.1643	-2	52	53	529.2398	10
61	62	531.6180	6	59	60	528.1149	-1	51	52	530.1493	-4
60	61	532.5798	16	58	59	529.0610	-3	50	51	531.0557	-5
59	60	533.5362	14	57	58	530.0035	1	49	50	531.9600	15
58	59	534.4843	-30	56	57	530.9413	-0	48	49	532.8551	-15
57	58	535.4336	-19	54	55	532.8039	-6	46	47	534.6393	-6
56	57	536.3776	-19	52	53	534.6511	3	45	46	535.5265	14
55	56	537.3200	8	51	52	535.5688	12	43	44	537.2817	-8
54	55	538.2546	-2	50	51	536.4809	9	42	43	538.1559	12
52	53	540.1156	26	49	50	537.3876	-6	41	42	539.0226	-0
51	52	541.0361	4	48	49	538.2916	-6	40	41	539.8844	-18
50	51	541.9523	-18	47	48	539.1909	-9	39	40	540.7449	-4
48	49	543.7787	6	46	47	540.0865	-6	38	39	541.6017	16
47	48	544.6810	-26	45	46	540.9806	25	37	38	542.4514	9
46	47	545.5818	-29	44	45	541.8651	3	36	37	543.2964	-1
45	46	546.4810	-6	43	44	542.7467	-4	35	36	544.1387	7
44	45	547.3747	7	42	43	543.6247	-4	34	35	544.9746	-6
43	44	548.2630	8	41	42	544.4984	-3	33	34	545.8067	-12
42	43	549.1449	-9	40	41	545.3675	-5	32	33	546.6365	3
41	42	550.0247	-5	39	40	546.2323	-4	31	32	547.4584	-16
40	41	550.9005	4	38	39	547.0921	-11	30	31	548.2807	13
39	40	551.7710	4	37	38	547.9486	-6	29	30	549.0937	-6
38	39	552.6380	12	36	37	548.8031	23	28	29	549.9037	-10
37	38	553.4976	-9	35	36	549.6477	-3	27	28	550.7121	16
36	37	554.3560	3	34	35	550.4902	-5	26	27	551.5117	-1
35	36	555.2084	-1	33	34	551.3294	4	25	26	552.3073	-14
34	35	556.0572	4	32	33	552.1631	3	24	25	553.1009	-2
33	34	556.9026	19	31	32	552.9911	-11	23	24	553.8894	6
32	33	557.7398	-2	30	31	553.8150	-20	22	23	554.6724	4
30	31	559.4069	17	29	30	554.6349	-24	21	22	555.4524	18
29	30	560.2305	-5	28	29	555.4524	-7	20	21	556.2247	0
28	29	561.0524	1	27	28	556.2659	14	19	20	556.9936	-5
27	28	561.8699	9	26	27	557.0721	9	18	19	557.7587	-3
26	27	562.6840	27	25	26	557.8728	-6	17	18	558.5215	23
25	26	563.4890	2	24	25	558.6713	1	15	16	560.0265	7
24	25	564.2923	4	23	24	559.4645	2	14	15	560.7707	-14
23	24	565.0905	1	22	23	560.2540	13	11	12	562.9818	-14
22	23	565.8851	8	21	22	561.0371	4	9	10	564.4331	-6
21	22	566.6717	-18	20	21	561.8170	10	5	6	567.2779	-2
19	20	568.2360	-21	19	20	562.5896	-11	5	4	574.7037	-16
18	19	569.0129	-5	18	19	563.3611	3	7	6	575.9949	23
17	18	569.7839	-2	17	18	564.1259	-4	8	7	576.6275	-15
11	12	574.3110	11	16	17	564.8870	-1	9	8	577.2577	-27
9	10	575.7851	43	15	16	565.6445	12	10	9	577.8839	-29
8	9	576.5105	15	13	14	567.1410	-5	11	10	578.5058	-26
7	8	577.2305	-21	7	6	581.7221	-14	12	11	579.1259	9
5	6	578.6629	-23	11	10	584.2581	3	14	13	580.3445	14
4	5	579.3714	-30	12	11	584.8796	6	16	15	581.5390	-25

TABLE II—Continued

N	N''	Observed	Δ	N	N''	Observed	Δ	N	N''	Observed	Δ
6	5	586.8548	-1	13	12	585.4946	-6	17	16	582.1329	-3
13	12	591.3029	-24	14	13	586.1094	31	18	17	582.7201	3
16	15	593.1375	-1	15	14	586.7148	22	20	19	583.8790	11
17	16	593.7408	26	16	15	587.3113	-24	21	20	584.4499	5
18	17	594.3330	-8	17	16	587.9104	5	22	21	585.0161	2
19	18	594.9259	15	18	17	588.5013	3	23	22	585.5780	8
20	19	595.5097	-1	19	18	589.0861	-9	24	23	586.1336	1
21	20	596.0912	10	20	19	589.6679	-1	25	24	586.6872	25
22	21	596.6642	-12	21	20	590.2443	3	26	25	587.2320	13
23	22	597.2350	-5	22	21	590.8149	1	27	26	587.7707	-9
24	23	597.7996	-9	23	22	591.3821	16	28	27	588.3082	8
26	25	598.9147	-4	24	23	591.9407	-4	29	28	588.8393	12
27	26	599.4651	5	25	24	592.4969	3	30	29	589.3636	0
29	28	600.5491	8	26	25	593.0493	23	31	30	589.8852	13
30	29	601.0828	6	27	26	593.5918	-4	32	31	590.3995	4
31	30	601.6091	-19	28	27	594.1310	-13	33	32	590.9089	-1
32	31	602.1345	-1	29	28	594.6669	-3	34	33	591.4142	3
33	32	602.6517	-12	30	29	595.1962	-8	35	34	591.9138	4
34	33	603.1665	5	31	30	595.7210	-5	36	35	592.4074	-4
35	34	603.6740	1	32	31	596.2426	17	37	36	592.8969	0
36	35	604.1772	8	33	32	596.7541	-10	38	37	593.3812	4
37	36	604.6743	5	34	33	597.2640	1	39	38	593.8597	4
38	37	605.1653	-5	35	34	597.7669	-7	40	39	594.3330	3
39	38	605.6527	1	36	35	598.2670	9	41	40	594.8023	15
40	39	606.1344	5	37	36	598.7597	4	42	41	595.2640	5
41	40	606.6100	-0	38	37	599.2481	9	43	42	595.7210	1
42	41	607.0808	1	39	38	599.7296	-3	44	43	596.1735	3
43	42	607.5474	13	40	39	600.2073	1	45	44	596.6191	-9
44	43	608.0066	4	41	40	600.6801	8	46	45	597.0626	11
45	44	608.4599	-10	42	41	601.1464	3	47	46	597.4976	0
46	45	608.9104	2	43	42	601.6091	16	48	47	597.9289	5
47	46	609.3522	-20	44	43	602.0624	-11	49	48	598.3559	21
48	47	609.7927	0	45	44	602.5144	1	50	49	598.7746	7
49	48	610.2263	6	46	45	602.9605	8	51	50	599.1886	0
50	49	610.6537	3	47	46	603.3976	-21	52	51	599.5981	3
51	50	611.0754	-3	48	47	603.8344	0	54	53	600.3979	-21
52	51	611.4922	-3	49	48	604.2642	6	55	54	600.7924	-6
53	52	611.9035	-4	50	49	604.6877	2	56	55	601.1800	-6
54	53	612.3109	12	51	50	605.1068	9	57	56	601.5634	8
55	54	612.7105	4	52	51	605.5179	-10	58	57	601.9390	-1
56	55	613.1046	-4	53	52	605.9270	5	59	58	602.3098	-5
57	56	613.4937	-7	54	53	606.3295	9	60	59	602.6759	1
58	57	613.8782	-1	55	54	606.7261	9	61	60	603.0353	-7
59	58	614.2576	9	56	55	607.1171	6	62	61	603.3882	-24
60	59	614.6293	-1	57	56	607.5012	-10	63	62	603.7391	-6
61	60	614.9971	3	58	57	607.8823	-1	64	63	604.0830	-2
62	61	615.3585	1	59	58	608.2571	-0	65	64	604.4211	-1
63	62	615.7142	-4	60	59	608.6266	3	66	65	604.7521	-16
64	63	616.0624	-28	61	60	608.9903	3	67	66	605.0800	-4
65	64	616.4104	4	62	61	609.3522	40	68	67	605.4035	18
66	65	616.7491	-4	63	62	609.7002	-5	69	68	605.7187	13
67	66	617.0816	-16	64	63	610.0475	-3	70	69	606.0269	-5
68	67	617.4105	-8	65	64	610.3894	2	71	70	606.3295	-25
69	68	617.7327	-11	66	65	610.7253	2	72	71	606.6309	2
70	69	618.0509	3	67	66	611.0552	-1	73	72	606.9231	-8
71	70	618.3627	10	68	67	611.3805	5	74	73	607.2124	9
72	71	618.6664	-8	69	68	611.6988	-2	76	75	607.7689	-6
73	72	618.9674	4	70	69	612.0113	-12	77	76	608.0395	-5
74	73	619.2590	-21	71	70	612.3210	7	78	77	608.3041	-7
75	74	619.5485	-9	72	71	612.6242	18	79	78	608.5639	-0

TABLE II—Continued

N'	N''	Observed	Δ	N'	N''	Observed	Δ	N'	N''	Observed	Δ
21	22	549.9129	-18	3	4	557.4708	37	16	15	564.5263	-31
20	21	550.6845	11	1	0	560.8229	39	17	16	565.1062	-16
19	20	551.4468	-9	5	4	563.4128	-15	18	17	565.6766	-45
18	19	552.2048	-25	7	6	564.6887	58	21	20	567.3681	-32
16	17	553.7123	-4	8	7	565.3131	32	22	21	567.9249	2
15	16	554.4596	11	11	10	567.1584	-33	23	22	568.4702	-29
14	15	555.1998	1	14	13	568.9665	-27	24	23	569.0129	-36
13	14	555.9362	-1	15	14	569.5570	-49	25	24	569.5570	21
12	13	556.6689	7	24	23	574.6717	4	35	34	574.6589	-1
11	12	557.3942	-13	25	24	575.2146	7	36	35	575.1409	-3
10	11	558.1205	25	26	25	575.7526	11	37	36	575.6184	1
6	7	560.9607	-7	27	26	576.2871	32	38	37	576.0899	-3
15	14	575.2296	17	28	27	576.8110	-2	39	38	576.5574	5
16	15	575.8209	8	29	28	577.3324	-11	40	39	577.0195	11
17	16	576.4076	4	30	29	577.8498	-8	41	40	577.4753	6
18	17	576.9897	3	31	30	578.3661	34	42	41	577.9267	9
19	18	577.5654	-12	32	31	578.8693	-2	43	42	578.3751	36
20	19	578.1388	1	33	32	579.3714	1	44	43	578.8121	-1
21	20	578.7062	4	34	33	579.8684	5	45	44	579.2479	4
22	21	579.2693	14	35	34	580.3608	16	46	45	579.6771	-4
23	22	579.8273	24	36	35	580.8444	-11	47	46	580.1011	-12
24	23	580.3762	-6	37	36	581.3270	4	48	47	580.5229	10
25	24	580.9235	-2	38	37	581.8021	-3	49	48	580.9409	49
26	25	581.4665	10	39	38	582.2734	4	50	49	581.3452	3
27	26	582.0013	-9	40	39	582.7388	4	51	50	581.7493	8
28	27	582.5360	23	41	40	583.1966	-20	52	51	582.1472	5
29	28	583.0592	-9	42	41	583.6540	5	54	53	582.9285	14
30	29	583.5813	-1	43	42	584.1003	-29	55	54	583.3050	-42
31	30	584.1003	27	44	43	584.5449	-27	56	55	583.6865	6
32	31	584.6091	5	45	44	584.9852	-15	57	56	584.0578	5
33	32	585.1164	19	46	45	585.4207	2	58	57	584.4230	-3
34	33	585.6147	-5	47	46	585.8493	2	59	58	584.7861	22
35	34	586.1094	-12	48	47	586.2736	13	60	59	585.1400	10
36	35	586.6012	3	49	48	586.6877	-25	61	60	585.4946	59
37	36	587.0854	-6	50	49	587.1023	-4	62	61	585.8330	1
38	37	587.5654	-4	51	50	587.5097	-3	63	62	586.1716	-1
39	38	588.0413	10	52	51	587.9104	-14	64	63	586.5045	-6
40	39	588.5099	1	53	52	588.3082	-1	65	64	586.8334	4
41	40	588.9723	-15	54	53	588.7000	6	66	65	587.1552	-1
42	41	589.4320	-6	55	54	589.0861	11	67	66	587.4722	0
43	42	589.8852	-10	56	55	589.4652	-2	68	67	587.7849	13
44	43	590.3352	7	57	56	589.8401	-2	69	68	588.0892	-2
45	44	590.7776	2	58	57	590.2083	-14	70	69	588.3879	-18
46	45	591.2144	-7	59	58	590.5739	2	72	71	588.9723	-13
47	46	591.6479	5	60	59	590.9320	-4	74	73	589.5331	-23
48	47	592.0754	10	61	60	591.2862	7	75	74	589.8094	16
49	48	592.4969	9	62	61	591.6335	4	77	76	590.3352	-7
50	49	592.9125	2	63	62	591.9742	-12	78	77	590.5894	-21
51	50	593.3220	-12	64	63	592.3121	1	81	80	591.3231	-14
52	51	593.7292	5	65	64	592.6426	-6	82	81	591.5573	-3
53	52	594.1310	22	66	65	592.9668	-20	89	88	593.0298	5
54	53	594.5246	10	67	66	593.2888	-3	91	90	593.3981	0
55	54	594.9139	10	68	67	593.6035	-1	92	91	593.5744	6
56	55	595.2947	-22	69	68	593.9109	-19	93	92	593.7408	-31
57	56	595.6738	-14	70	69	594.2166	4	94	93	593.9109	28
58	57	596.0467	-16	73	72	595.0943	10	96	95	594.2166	-23
59	58	596.4172	13	74	73	595.3759	15	100	99	594.7721	14
61	60	597.1336	-9	75	74	595.6507	7	102	101	595.0093	-21
62	61	597.4862	6	76	75	595.9183	-16	107	106	595.5097	-1
63	62	597.8304	-9	77	76	596.1849	7				

TABLE II—Continued

<i>N'</i>	<i>N''</i>	Observed	Δ	<i>N'</i>	<i>N''</i>	Observed	Δ	<i>N'</i>	<i>N''</i>	Observed	Δ
64	63	598.1703	-10	78	77	596.4432	4				
65	64	598.5084	25	79	78	596.6960	2				
66	65	598.8356	6	80	79	596.9407	-25				
67	66	599.1566	-17	81	80	597.1859	11				
68	67	599.4770	7	82	81	597.4168	-40				
69	68	599.7879	-7	83	82	597.6493	-17				
70	69	600.0926	-29	84	83	597.8770	14				
71	70	600.3979	13	86	85	598.3094	20				
72	71	600.6928	6	89	88	598.9147	26				
73	72	600.9805	-16	92	91	599.4651	4				
75	74	601.5456	5	94	93	599.8042	0				
76	75	601.8187	5	99	98	600.5491	-13				
78	77	602.3477	5	100	99	600.6801	-19				
80	79	602.8550	14	101	100	600.8087	10				
81	80	603.0981	-1	104	103	601.1464	-30				
82	81	603.3328	-43	112	111	601.8004	25				
85	84	604.0186	-8								
90	89	605.0387	-25								
94	93	605.7530	-10								
96	95	606.0756	4								
100	99	606.6460	-12								
103	102	607.0142	4								
116	115	607.9793	5								
118	117	608.0395	32								
7 6 Band				8 7 Band							
18	19	535.8498	-29	16	17	531.9600	-46				
15	16	538.0617	40	13	14	534.1317	48				
14	15	538.7899	64	9	10	536.9443	-18				
10	11	541.6454	42	7	8	538.3268	-13				
7	8	543.7294	-65	3	4	541.0361	-3				
3	2	551.0509	-52	2	3	541.7102	84				
8	7	554.1877	-55	4	3	546.2323	44				
9	8	554.8083	21	9	8	549.3116	-66				
13	12	557.2067	-28	12	11	551.1111	-34				
15	14	558.3828	9	16	15	553.4411	-6				
16	15	558.9603	-4	24	23	557.8630	30				
17	16	559.5356	10	27	26	559.4362	13				
20	19	561.2244	-23	29	28	560.4609	13				
24	23	563.4128	-3	30	29	560.9607	-38				
25	24	563.9467	-5	33	32	562.4489	2				
26	25	564.4775	12	35	34	563.4128	1				
31	30	567.0448	-13	36	35	563.8939	68				
33	32	568.0429	45	37	36	564.3583	19				
34	33	568.5302	33	38	37	564.8213	9				
35	34	569.0129	26	39	38	565.2807	14				
37	36	569.9572	-45	40	39	565.7276	-56				
47	46	574.4079	6	41	40	566.1817	-1				
48	47	574.8211	-20	46	45	568.3498	28				
50	49	575.6416	28	47	46	568.7653	9				
52	51	576.4328	-5	48	47	569.1729	-37				
53	52	576.8214	-12	50	49	569.9814	-36				
55	54	577.5853	1	64	63	575.0491	5				
56	55	577.9573	-11	65	64	575.3664	-35				
57	56	578.3247	-15	66	65	575.6828	-29				
58	57	578.6934	46	67	66	575.9949	-12				
59	58	579.0475	16	70	69	576.8930	-15				
60	59	579.3982	6	72	71	577.4632	-27				
61	60	579.7411	-29	73	72	577.7416	-17				

TABLE II—Continued

N'	N''	Observed	Δ	N'	N''	Observed	Δ	N'	N''	Observed	Δ
62	61	580.0835	-13	75	74	578.2780	-36				
63	62	580.4225	22	76	75	578.5441	17				
64	63	580.7512	9	77	76	578.7990	14				
65	64	581.0737	-11	78	77	579.0475	2				
66	65	581.3934	-6	79	78	579.2902	-11				
67	66	581.7102	26	80	79	579.5373	74				
68	67	582.0140	-17	81	80	579.7639	12				
71	70	582.9101	29								
72	71	583.1966	34								
75	74	584.0193	11								
76	75	584.2843	23								
77	76	584.5449	45								
82	81	585.7463	-13								
84	83	586.1938	28								
85	84	586.4028	-14								
88	87	587.0081	-16								
91	90	587.5654	15								

(5 Torr) was then introduced to prevent any deposition of solid material onto the KRS-5 cell windows. The high-resolution spectrum was recorded at a resolution of 0.01 cm^{-1} over the spectral range $350\text{--}750 \text{ cm}^{-1}$ with a liquid-helium-cooled Si:B detector and a KBr beamsplitter. The upper limit of 750 cm^{-1} was set by a cold filter attached to the detector, while a combination of detector response and KBr beamsplitter transmission effectively set the lower limit to 350 cm^{-1} . The final spectrum consisted of 100 coadded scans. A portion of the spectrum showing part of the R branches of the first few bands can be seen in Fig. 1.

RESULTS

Rotational lines were measured using PC-DECOMP, a spectral analysis program written by J. Brault, which fits the line profiles with Voigt lineshape functions. Assignment of the CaF bands was performed using an interactive color Loomis-Wood program. The overall spectrum of CaF was then calibrated with respect to pure rotational HF lines (17) which were present as an impurity. Although CaF has a ${}^2\Sigma^+$

TABLE III
Spectroscopic Constants for the $X^2\Sigma^+$ Ground State of CaF (in cm^{-1})

v	T_v	B_v	$10^7 D_v$
0	0	0.342488337(90)	4.68963(90)
1	582.847759(110)	0.340053845(52)	4.69073(85)
2	1159.946892(192)	0.337629480(50)	4.69135(82)
3	1731.34856(21)	0.335215331(50)	4.69150(79)
4	2297.10325(27)	0.332811563(112)	4.69110(77)
5	2857.26144(37)	0.330418358(181)	4.69019(77)
6	3411.87316(45)	0.32803600(23)	4.68889(76)
7	3960.98951(61)	0.32566419(35)	4.68674(84)
8	4504.65944(73)	0.32330425(51)	4.68533(98)

ground state, no spin-rotation splitting was observed; therefore, data reduction was performed by fitting the data to the conventional Dunham expression

$$E(v, N) = \sum_{ij} Y_{ij} \left(v + \frac{1}{2} \right)^i [N(N+1)]^j.$$

The microwave lines (10) were corrected for the effects of fine and hyperfine structure and were added to the fit. The Dunham coefficients obtained are shown in Table I. The equilibrium internuclear distance of 1.9516386(35) Å was calculated from the Y_{01} Dunham coefficient and found to be in agreement with that reported by Dulick *et al.*, (4). The infrared rovibrational line positions are found in Table II, and spectroscopic constants for the $X^2\Sigma^+$ ground state of CaF are given in Table III.

RECEIVED: November 22, 1994

REFERENCES

1. R. W. FIELD, D. O. HARRIS, AND T. TANAKA, *J. Mol. Spectrosc.* **57**, 107-117 (1975).
2. J. NAKAGAWA, P. J. DOMAILLE, T. C. STEIMLE, AND D. O. HARRIS, *J. Mol. Spectrosc.* **70**, 374-385 (1978).
3. P. F. BERNATH, P. G. CUMMINS, AND R. W. FIELD, *Chem. Phys. Lett.* **70**, 618-620 (1980).
4. M. DULICK, P. F. BERNATH, AND R. W. FIELD, *Can. J. Phys.* **58**, 703-712 (1980).
5. W. E. ERNST, J. KÄNDLER, AND O. KNÜPPEL, *J. Mol. Spectrosc.* **153**, 81-90 (1992).
6. P. F. BERNATH AND R. W. FIELD, *J. Mol. Spectrosc.* **82**, 339-347 (1980).
7. J. VERGÈS, C. EFFANTIN, A. BERNARD, A. TOPOUZKHANIAN, A. R. ALLOUCHE, J. D'INCAN, AND R. F. BARROW, *J. Phys. B: At. Mol. Opt. Phys.* **26**, 279-284 (1993).
8. W. J. CHILDS, L. S. GOODMAN, U. NIELSEN, AND V. PFEUFER, *J. Chem. Phys.* **80**, 2283-2287 (1984).
9. W. J. CHILDS AND L. S. GOODMAN, *Phys. Rev. Lett.* **44**, 316-319 (1980).
10. W. J. CHILDS, G. L. GOODMAN, AND L. S. GOODMAN, *J. Mol. Spectrosc.* **86**, 365-392 (1981).
11. L. M. ZIURYS, A. J. APPONI, AND T. G. PHILLIPS, *Astrophys. J.* **433**, 729-732 (1994).
12. M. A. ANDERSON, M. D. ALLEN, AND L. M. ZIURYS, *Astrophys. J.* **424**, 503-506 (1994).
13. J. E. MURPHY, J. M. BERG, A. J. MERER, N. A. HARRIS, AND R. W. FIELD, *Phys. Rev. Lett.* **65**, 1861-1864 (1990).
14. N. A. HARRIS AND R. W. FIELD, *J. Chem. Phys.* **98**, 2642-2646 (1993).
15. J. M. BERG, J. E. MURPHY, N. A. HARRIS, AND R. W. FIELD, *Phys. Rev. A* **48**, 3012-3029 (1993).
16. Z. J. JAKUBEK, N. A. HARRIS, R. W. FIELD, J. A. GARDNER, AND E. MURAD, *J. Chem. Phys.* **100**, 622-627 (1994).
17. R. B. LEBLANC, J. B. WHITE, AND P. F. BERNATH, *J. Mol. Spectrosc.* **164**, 574-579 (1994).